A Nonradiative Dielectric Waveguide Based Wideband Reflectarray Antenna

WEN WU
Department of Communications Engineering
Tohoku University
Sendai, 980-8579 Japan
ORCID: 0000-0002-9352-9805

Qiang Chen
Department of Communications Engineering
Tohoku University
Sendai, 980-8579 Japan
ORCID: 0000-0001-8714-6819

2024 IEEE International Workshop on Antenna Technology (iWAT) | 979-8-3503-1475-5/24/$31.00 ©2024 IEEE | DOI: 10.1109/iWAT57102.2024.10535813

***Abstract*—This paper introduces the design of a reflectarray antenna (RA) based on a nonradiative dielectric (NRD) waveguide. The proposed design achieves wideband performance by eliminating the need for traditional resonant components. Unstable reflection coefficient of the element under oblique incidence is investigated and addresses through a specific feed configuration. The 16×16 RA prototype exhibits a verified capability for maximum collimation beam angles up to 60°, accompanied by a gain variation of under 1.5 dB within the frequency range of 9.5 GHz to 11.5 GHz, with relative low beam squint.**

Keywords—Nonradiative Dielectric(NRD) Waveguide, Reflectarray Antenna, Wideband

I. Introduction

Wideband reflectarray antennas (RAs) have garnered significant attention in research, particularly for satellite communication(SATCOM) and 5G/B5G applications [1][2]. Many studies have utilized broadband resonant elements with rotating or complementary structures fabricated using printed circuit board (PCB) technology to achieve broad radiation performance[3]-[5]. Nevertheless, these structures often incorporate multiple resonators, leading to a significant increase in metal loss, particularly when operating in the millimeter-wave.

Waveguides can serve as potential broadband RA elements due to their non-resonant properties[6][7]. However, their transmission line mode leads to high profile heights. Moreover, the periodic of RA element should be larger than one-half the wavelength of the lowest operating frequency. This makes them unsuitable for applications requiring large collimation angles, considering the risk of grating lobes. The non-radiative dielectric (NRD) waveguide[8][9] is a highly compact waveguide containing a dielectric slab and can serve as a potential element in wideband RA design using the time delay line approach.

In this paper, a wideband NRD waveguide based RA is proposed. The propagation mode of NRD waveguide element and the performance of the RA at the maximum collimated angle are investigated. The required phase distribution of the collimated beam is achieved by changing the dimensions of the dielectric slab in the propagation direction. Simulation results show that the proposed design maintains a wide gain bandwidth and low beam squint.

II. NRD Waveguide Element for Proposed Wideband RA

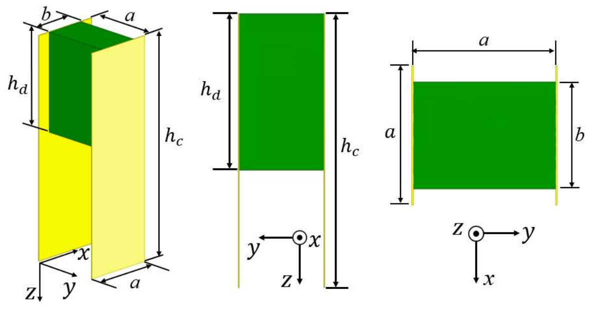

Fig. 1. Proposed NRD waveguide element structure. (a) Diagram. (b) Front view. (c) Top view. Yellow represents metal, and green represents dielectric slab.

A. Proposed NRD waveguide structure and propagation mode

The construction of the proposed NRD waveguide as an RA element is depicted in Fig. 1. It consists of a dielectric slab with cross-sectional dimensions $a \times b$ and height h_d, sandwiched between parallel metal walls. By introducing a dielectric constants gap between the dielectric slab and surrounding air, electromagnetic waves are confined within the dielectric slab. This modification significantly reduces the cutoff frequency of the NRD waveguide compared to a rectangular waveguide with the same cross-sectional size of $a \times b$.

The propagation modes include two types: longitudinal-section-magnetic (LSM) and longitudinal-section-electric (LSE)[9], as shown in Fig.2. To minimize power loss on the metallic walls, the fundamental LSM mode (LSM_{11}), whose magnetic field is parallel to the longitudinal plane (*xoz* plane), is set as the dominant mode and the fundamental LSE mode (LSE_{11}) should be operated as a parasitic mode. In this configuration, the incident wave is polarized in the x-direction. The significant portion of the transverse component of the electric field in the LSM11 mode aligns parallel to the electric field of the incident wave, facilitating efficient excitation of the NRD waveguide. In contrast, the transverse component of the LSE_{11} mode's electric field is orthogonal to the polarization direction of the incident wave, making it difficult to couple to the waveguide and be excited. As a result, only the LSM11 mode is efficiently excited when the *x*-polarization wave is incident at the open end of the NRD waveguide.

Due to the confinement of the incident wave within the dielectric slab, the reflection phase can be tuned by the propagation length, which is determined by the height of the

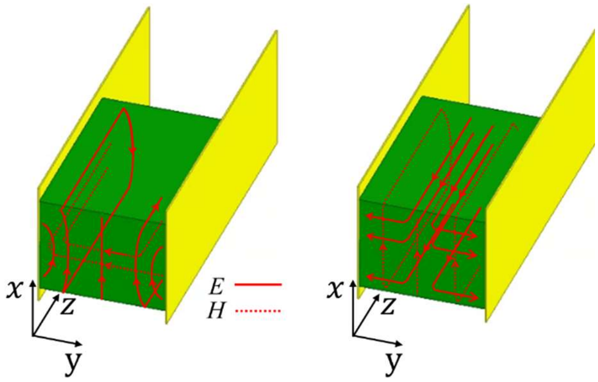

(a) (b)

Fig. 2. Fundamental propagation modes of NRD waveguide. (a) LSM_{11}, (b) LSE_{11}

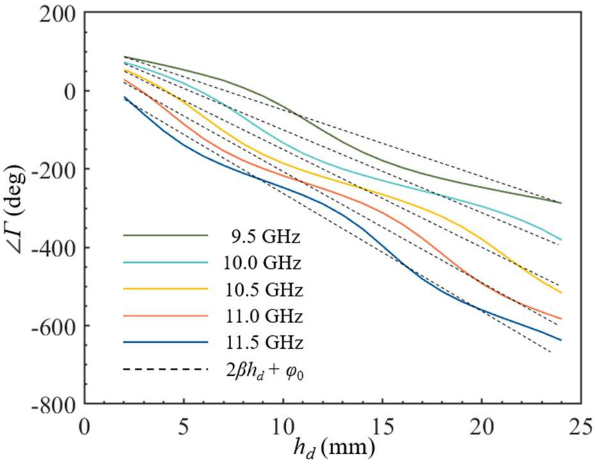

Fig. 3. Simulated reflection phase versus h_d for different frequencies.

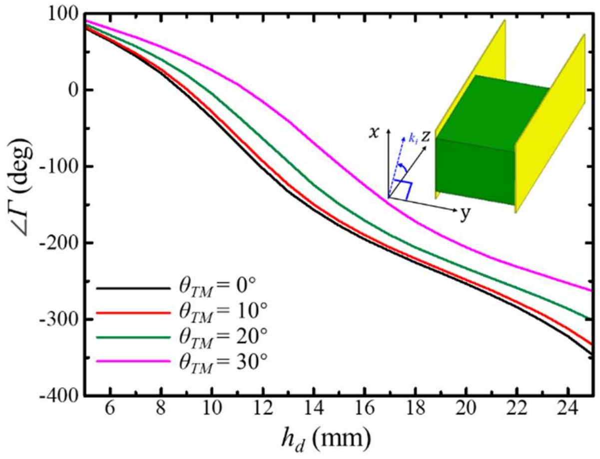

(a)

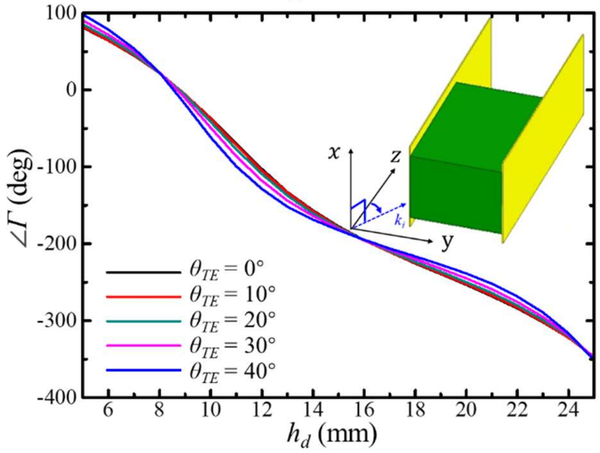

(b)

Fig. 4. Simulated phase of reflection coefficient at 10.5 GHz under oblique incidence for (a) TE mode and (b) TM mode.

dielectric slab (h_d). To verify the phase-tuning ability, simulations are conducted using Floquet port excitation with periodic boundary conditions. The results for varying the height of the dielectric slab(h_d) are illustrated in Fig. 3. Under normal incidence, the obtained reflection phase is proportional to the value of h_d and can be approximately to a linear function. The slope of this linear function is equivalent to twice the propagation constant (2β) at each frequency.

B. Performance under Oblique Incidence

The performance of the proposed NRD structure under oblique incidence, resulting from the spatial feed, is investigated by simulation. For the TE mode, the propagation direction of the oblique incident wave is parallel to the *yoz* plane, while for the TM mode, the propagation is parallel to the *xoz* plane, as shown in Fig.4.It can be observed that the reflection phase of TE mode incidence remains relatively stable, with a maximum variation of 25°, even at oblique incidence angles of up to 40°. However, in Fig. 4(b), for TM mode incidence, the phase variation becomes more pronounced. It exceeds 100° when the incidence angle reaches 30°. This behavior can be attributed to the absence of metal walls along the polarization direction in the nonradiative dielectric (NRD) waveguide, which impedes the suppression of parasitic LSE11 modes. Consequently, the dominant LSM11 mode undergoes mode degeneracy, particularly at larger oblique angles. In the case of TM mode incidence, the electric field exhibits both transverse and longitudinal components. Notably, the longitudinal electric field component (*Ez*) strengthens as the angle increases. While, for the LSM11 mode, *Ez* is expected to be significantly weaker (about -25 dB) compared to the transverse component Ex, at an incidence angle of 30°, *Ez* would be -2.3 dB (tan30°). This magnitude is sufficient to excite the LSE_{11} mode, leading to a varied reflection phase due to the presence of multiple modes. To address the unstable reflection phase under oblique incident angles, optimization of the feed configuration is performed. This optimization not only ensures high efficiency but also limits the incidence angle for TM mode to less than 20°.The detail analysis will be described in following section.

III. RA Design and Performance

A 16 × 16 element prototype of the NRD waveguide RA is carefully designed in order to evaluate the maximum angle of collimated beam scanning. A 15 dBi standard gain horn was chosen for the feed antenna, a choice that took into account both the feed volume limitation and the high focal-to-diameter (F/D) ratio required. The power pattern matching function of the feed is given by $\cos^{2q}(\theta)$,where q value is 14. By using the values of q and F/D, the illumination efficiency (η_i)and the spillover efficiency (η_s) can be calculated [10]. The aperture efficiency (η_a) can then be obtained by multiple the η_i and η_s.The calculated results are depicted in Fig. 5, showing that the aperture efficiency (AE) reaches a maximum of 74.9% when the F/D value is set to 1.22.

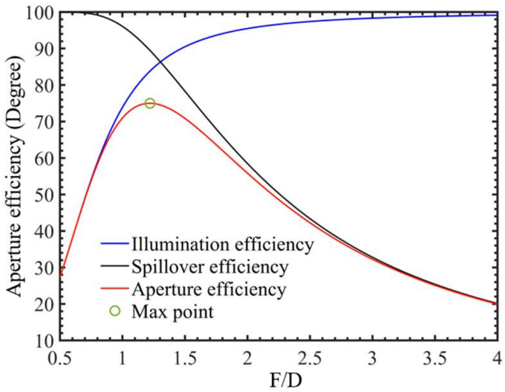

Fig. 5 Calculated RA efficiency for different values of F/D based on the employed 15 dBi feed antenna.

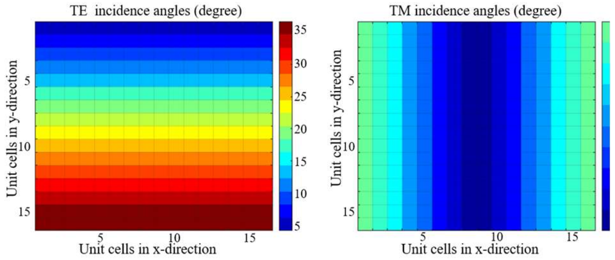

(a) (b)

Fig. 6 The oblique incident angles based on the proposed feed configuration. (a) TE mode incidence component. (b) TM mode incidence component.

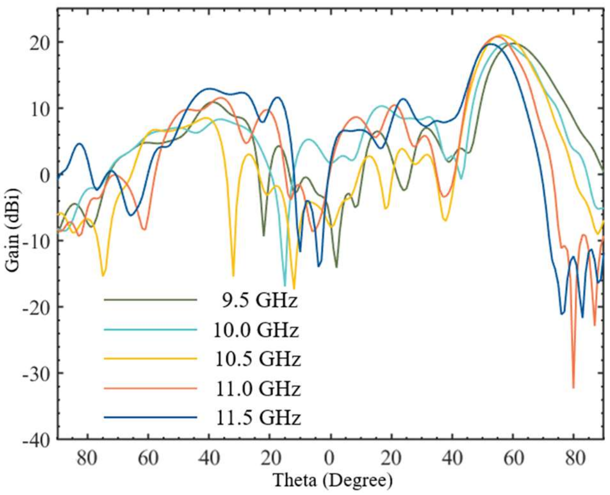

Fig. 7 Proposed RA gain with collimated beam at 60 degree

It's noteworthy that when adjusting the F/D value between 1.0 and 1.5, the aperture efficiency exhibits a variation within 5%. For the proposed design, the value of F/D is set to 1.22 and the feed is offset 20° to the broadside on the *yoz* plane. Each cell's incidence angle can be decomposed into TE mode and TM mode, which propagate parallel to the *yoz* and *xoz* planes, respectively. The proposed offset-fed configuration not only reduces the aperture blockage effect but also plays a crucial role in achieving a smaller angle for the TM mode oblique incidence component. As illustrated in Fig. 6, the distribution of TE mode and TM mode components on the RA aperture reveals that the TE mode component has a maximum incidence angle of 35° at the y-direction edge, while the TM mode component is symmetrically distributed in the x-direction, reaching a maximum angle of 18° at both edges. Consequently, the variation in reflection phase induced by oblique incident waves remains below 30°. Furthermore, the power taper in the x-direction is -10 dB, and in the y-direction, it is -12 dB and -8 dB, respectively. The collimation beam is designed with an angle θ= 60° ,Φ= 90°. The required phase for each element is achieved by selecting an appropriate height for the dielectric slab, h_d, as depicted in Fig. 3. The simulated gain is illustrated in Fig. 7, showing a gain variation of under 1.5 dB between 9.5 to 11.5 GHz. The peak gain, occurring at 10.5 GHz, reaches 21 dBi. The highest side lobe level (SLL) is -7.8 dB at 11.5 GHz. The maximum beam squint of 7° showcases significant advantages over other resonance element RAs[11].

IV. CONLUSION

The performance of the reflection coefficient for the Nonradiative Dielectric (NRD) waveguide RA element under oblique incident angles has been thoroughly investigated. The issues with an unstable phase response have been successfully addressed by implementing a specific feed configuration. With this optimized configuration, the proposed RA has demonstrated a large collimation beam angle, wide gain bandwidth, acceptable Side Lobe Level (SLL), and minimal beam squint.

REFERENCES

[1] E. Carrasco, J. A. Encinar and M. Barba, "Bandwidth Improvement in Large Reflectarrays by Using True-Time Delay," IEEE Transactions on Antennas and Propagation, vol. 56, no. 8, pp. 2496-2503, Aug. 2008.

[2] W. Wu, K. -D. Xu, Q. Chen, T. Tanaka, M. Kozai and H. Minami, "A Wideband Reflectarray Based on Single-Layer Magneto-Electric Dipole Elements With 1-bit Switching Mode," IEEE Transactions on Antennas and Propagation, vol. 70, no. 12, pp. 12346-12351, Dec.2022.

[3] R. Florencio, J. A. Encinar, R. R. Boix, V. Losada and G. Toso, "Reflectarray Antennas for Dual Polarization and Broadband Telecom Satellite Applications," IEEE Transactions on Antennas and Propagation, vol. 63, no. 4, pp. 1234-1246, April 2015.

[4] X. Li, X. Li, Y. Luo, G. Wei and X. Yi, "A Novel Single Layer Wideband Reflectarray Design Using Two Degrees of Freedom Elements," IEEE Transactions on Antennas and Propagation, vol. 69, no. 8, pp. 5095-5099, Aug. 2021.

[5] J. A. Encinar, "Design of two-layer printed reflectarrays using patches of variable size," IEEE Transactions on Antennas and Propagation, vol. 49, no. 10, pp. 1403-1410, Oct. 2001.

[6] Y. Liu, Y. J. Cheng, M. -H. Zhao and Y. Fan, "Dual-Band Shared-Aperture High-Efficiency Reflectarray Antenna Based on Structure-Reuse Technique," in IEEE Antennas and Wireless Propagation Letters, vol. 20, no. 3, pp. 366-370, March 2021,

[7] G. -B. Wu, Y. -S. Zeng, K. F. Chan, B. -J. Chen, S. -W. Qu and C. H. Chan, "High-Gain Filtering Reflectarray Antenna for Millimeter-Wave Applications," IEEE Transactions on Antennas and Propagation, vol. 68, no. 2, pp. 805-812, Feb. 2020.

[8] W. Wu, K. -D. Xu, Q. Chen, T. Tanaka, M. Kozai and H. Minami, "A Low-Cost Wideband Reflectarray Antenna Based on Nonradiative Dielectric Waveguide," IEEE Antennas and Wireless Propagation Letters, vol. 22, no. 12, pp. 3152-3156, Dec. 2023.

[9] F. Kuroki, K. Ikeda and T. Matsukawa, “Transmission characteristics of LSE/sub 01/ mode in high permittivity NRD guide,” Proceedings of 1997 Asia-Pacific Microwave Conf., vol.2, pp. 593-596, 1997.

[10] J. Huang and J. A. Encinar, Reflectarray Antennas. Hoboken-Piscataway, NJ, USA: Wiley—IEEE Press, 2007.

[11] H. Luyen, Z. Zhang, J. H. Booske and N. Behdad, "Wideband, Beam-Steerable Reflectarray Antennas Exploiting Electronically Reconfigurable Polarization-Rotating Phase Shifters," IEEE Transactions on Antennas and Propagation, vol. 70, no. 6, pp. 4414-4425, June 2022.